



Influence of lipid extraction and processing conditions on hydrothermal conversion of microalgae feedstocks – Effect on hydrochar composition, secondary char formation and phytotoxicity

Veronica Benavente^{a,*}, Sandra Lage^{b,c}, Francesco G. Gentili^b, Stina Jansson^a

^a Department of Chemistry, Umeå University, 90 187 Umeå, Sweden

^b Department of Forest Biomaterials and Technology, Swedish University of Agricultural Sciences, 901 83 Umeå, Sweden

^c Department of Environmental Science, Stockholm University, 106 91 Stockholm, Sweden

ARTICLE INFO

Keywords:

CO₂ capture systems
Hydrochar applications
Thermogravimetric analysis
Pyrolysis–gas chromatography/mass spectrometry analysis
Secondary char
Toxicity

ABSTRACT

This study investigated the effect of lipid extraction of microalgae feedstocks subjected to hydrothermal carbonization (HTC) with regard to the carbonization degree, chemical composition and phytotoxicity of hydrochars produced under different reaction temperatures and residence times. Special attention was given to the formation and composition of secondary char, as this part of the hydrochar may be of particular importance for environmental and technical applications. A microalgae polyculture grown in municipal wastewater was extracted to retrieve lipids, and both unextracted (MA) and extracted microalgae (EMA) were used to produce hydrochars at 180–240 °C for 1–4 h. The composition of the hydrochars was thoroughly characterized by elemental analysis, thermogravimetric analysis and pyrolysis–gas chromatography/mass spectrometry analysis. MA exhibited a greater carbonization degree than EMA and contained higher amounts of secondary char under the same processing conditions. During the carbonization of EMA, more decomposition products remained in the liquid phase and less polymerization occurred than for MA, which explained the lower solid yield of EMA-derived hydrochars in comparison to MA hydrochars. Consequently, although they contained potentially toxic substances (i.e., carboxylic acids, aldehydes and ketones), the EMA-derived hydrochars exhibited a lower phytotoxic potential. This indicates that low-temperature hydrochars containing less than 10% of extractives might be suitable as soil amendments, whereas extractive-rich hydrochars would be more appropriate for other long-term applications, such as adsorbents for contaminant removal, energy storage and composite materials. Detailed characterization of microalgae-derived hydrochars is required to enable the most suitable application areas to be identified for these materials, and thereby make full use of their function as carbon sinks.

1. Introduction

The application of microalgae-based wastewater treatment and CO₂ sequestration coupled with valuable biomass production has received extensive interest and research in the last few decades since it potentiates the restoration of environmental health and generation of feedstock for sustainable exploitation [1–3]. In comparison to forestry, agricultural biomass and aquatic plants, microalgae have approximately ten times higher growth rates and corresponding CO₂ fixation rates due to their energy-conserving structure [2]. Thus, they are an environmentally sustainable CO₂ capture alternative to the currently employed carbon capture and storage (CCS) technologies [2,4,5]. However, the final application of microalgae biomass will be decisive for this

technology to be truly considered a CCS system. Therefore, it is imperative to explore and develop sustainable uses of microalgae biomass that ensure long-lasting CO₂ capture systems that act as actual carbon sinks (Fig. 1).

Hydrothermal carbonization (HTC) is a promising technology for the conversion of sustainable organic waste streams to value-added products [6,7]. HTC is a wet, low-temperature thermochemical conversion process where the feedstock is heated to 180–275 °C in subcritical water to generate a carbon-enriched material called hydrochar. There is currently much interest in HTC because it has the potential to promote the desired waste management hierarchy prevalent in many countries regarding recovery and reuse of organic waste materials. Hydrochar has remarkable properties that make it an excellent substrate for a wide

* Corresponding author.

E-mail address: veronica.benavente@umu.se (V. Benavente).

<https://doi.org/10.1016/j.cej.2021.129559>

Received 21 January 2021; Received in revised form 21 March 2021; Accepted 24 March 2021

Available online 31 March 2021

1385-8947/© 2021 The Author(s). Published by Elsevier B.V. This is an open access article under the CC BY license (<http://creativecommons.org/licenses/by/4.0/>).

range of applications, including energy storage [7], environmental remediation [6,8] and renewable energy sources [9–11].

In the last decade, hydrothermal conversion of microalgae has mainly focused on the production of solid and liquid biofuels. In 2010, Heilmann et al. [12] were the first to investigate HTC of a variety of microalgae monoculture strains. They showed that microalgae are carbonized via dehydration into char products with energy contents in the bituminous coal range at 200 °C with reaction times as brief as 0.5 h. In the same year, Levine et al. [13] published a study in which HTC was integrated into a two-step technique for algal biodiesel production. The following year, Heilmann et al. [14] discussed the benefits of introducing the HTC process to microalgae biorefineries in the oil industry. Since then, several studies have investigated microalgae-derived hydrochar properties for subsequent energy applications [15–24]. However, the use of microalgae-derived hydrochars has barely been extended to application areas other than biofuel production. For example, only one study has explored their performance as adsorbents (hydrochars from commercial *Nannochloropsis* sp. for copper removal) [25]. Nevertheless, the results were promising and suggested that further research would be beneficial in this area. For hydrochars derived from microalgae polycultures grown in wastewater, the literature reflects a general scarcity of investigation.

Potential uses of microalgae-derived hydrochar other than as solid fuel include soil amendments, adsorbents for contaminant removal and energy storage, application areas that may serve as carbon sinks and contribute to mitigation of global warming. The applicability of hydrochars in these areas is strongly linked to their physicochemical properties, which vary considerably with the feedstock composition and severity of reaction conditions [9,16,26–28] and especially secondary char formation. Secondary char refers to the spherical structures that condense on the surface of primary char. This part of the hydrochar results from the aqueous phase degradation of biomass followed by polymerization of organic molecules into a solid phase [29] and possibly further carbonization by dehydration reactions [27]. Primary char, on the other hand, is the main hydrochar structure resulting from solid-solid conversion of the parent biomass, which retains the original morphology [29]. Secondary char confers a functional group-rich surface to the hydrochar, which makes the material very appealing for advanced applications, such as adsorption [25,30] and energy storage [31]. However, the formation of secondary char might also confer

phytotoxic properties that prevent application of the hydrochar to agricultural soils [32,33] despite possible benefits, mainly stimulated seedling growth [33].

The secondary char is extractable with organic solvents and comprises of predominantly organic acids, furfurals and phenols [28], which are produced in quantities and proportions that strongly depend on the initial composition of the feedstock and processing conditions [28,34]. Microalgae mainly consist of variable concentrations of carbohydrates, proteins and lipids. Among these, carbohydrates are the most prominent reactants contributing to secondary char formation [35,36] via degradation followed by re-polymerization mechanisms, as described in the literature [34]. Proteins can also assist in the growth phases of secondary char by the heterocyclic Maillard reaction with carbohydrates [37]. In contrast, lipids do not participate in char formation but hydrolyze to fatty acids that adsorb to the surface of the hydrochar [14,37]. Hydrochar-bound fatty acids are solvent extractable, and thus constitute the total solvent-extractable fraction of the hydrochar together with the secondary char. Complex matrices undergo complex reactions under HTC. The close relationship between lipids and secondary char as extractable substances deposited on the char surface suggests that lipids might have some effect on the carbonization of other components, and therefore formation of secondary char. Questions remain regarding the extent to which the extraction of lipids from microalgae prior to HTC affects the formation and characteristics of the secondary char, and in turn the suitability of microalgae-derived hydrochars for potential applications.

Investigations addressing these knowledge gaps are valuable for efficient utilization of all fractions in the microalgae-based value chain (Fig. S1). In an ideal microalgae-based system (i.e., microalgae-based wastewater treatment and CO₂ sequestration coupled with biomass production for subsequent exploitation), microalgae grown in local wastewater would first be allocated to an extraction procedure to recover valuable components (e.g., nutrients and lipids) [3,38]. Utilization of the microalgal biomass is highly dependent on the amount of wastewater micropollutants that accumulates in the microalgae during growth and bacteria. Thus, low-quality microalgae biomass with high amounts of contaminants and/or other organisms could not be used for resource recovery [3,38]. Neither the solid extraction residue nor the low-quality microalgae biomass are currently being utilized, but a bio-based economy demands maximized use of all resources and residuals

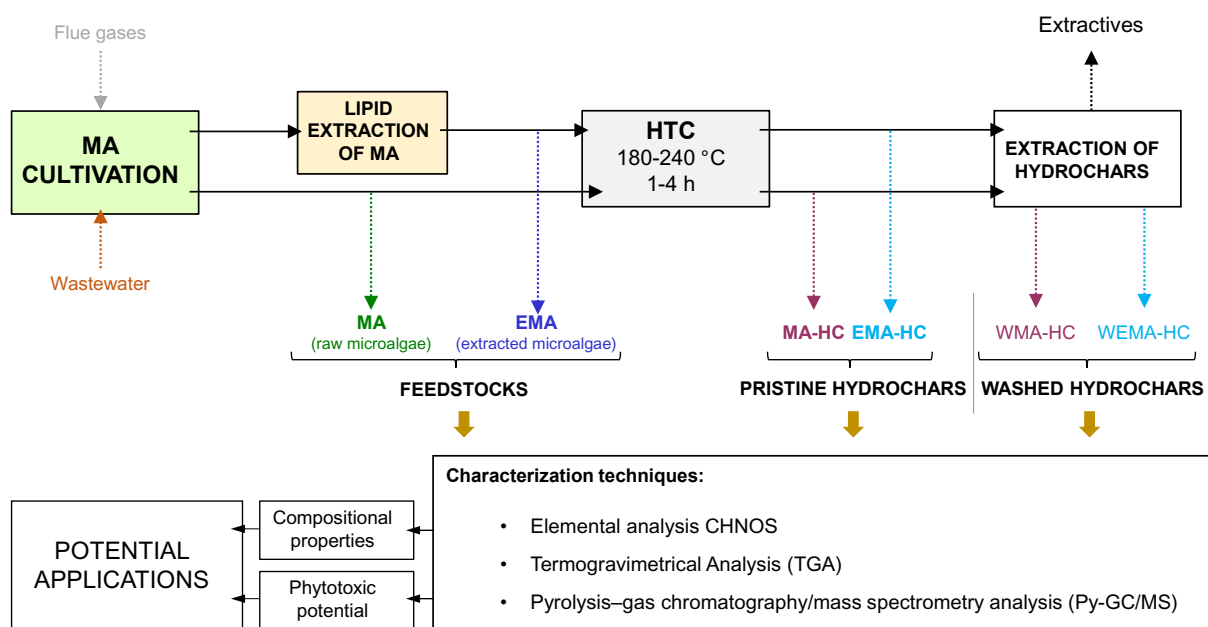


Fig. 1. Flow chart of the experimental method.

generated in different processes. There is therefore a demand for sustainable use of microalgae extraction residues and raw microalgae biomass not suitable for extraction. In this context, it is important to thoroughly characterize the carbonized microalgae residues vs. carbonized raw microalgae, which might exhibit different properties.

The present work aimed to study how the extraction of lipids influences the formation of secondary char during HTC of microalgae and the resulting hydrochar phytotoxicity under a wide range of HTC-processing conditions. The specific objectives were to (i) study the influence of temperature and residence time on mass yields and composition of hydrochars produced from an unextracted or lipid-extracted microalgae polyculture grown in municipal wastewater, (ii) investigate how HTC reaction conditions and the extraction of lipids affect the formation and characteristics of primary and secondary char by thermogravimetric analysis (TGA) and pyrolysis–gas chromatography/mass spectrometry analysis (Py-GC/MS), and (iii) evaluate the phytotoxicity of hydrochars and discuss utilization of microalgae-derived hydrochars with regard to the hydrochar properties. This study provides information essential for continued development of HTC as a sustainable process for production of hydrochar from microalgae biomass for environmental and technical applications.

2. Materials and methods

2.1. Materials

2.1.1. Chemicals

All chemicals used in this work were of analytical grade: dichloromethane (DCM) was purchased from Merck KGaA (Darmstadt, Germany), whereas hexane was purchased from Fischer Scientific (Göteborg, Sweden).

2.1.2. Microalgae polyculture

Microalgae were cultured in two raceway ponds 10 m long, 2 m wide and approximately 0.3 m deep with a surface area of 19.14 m² and volume of about 6 m³. The ponds were equipped with paddle wheels with six blades and were located outdoors at the Umeå Energi combined heat and power plant CHP-plant (Umeå, Sweden) during the 2017 summer season. The untreated municipal wastewater influent was collected from the local wastewater treatment plant (Vakin, Umeå). Flue gases from the CHP-plant, which incinerates both municipal and industrial solid wastes, were bubbled into the microalgae culture using gas diffusers (Cole Parmer, USA). The flue gases containing approximately 10% CO₂ (v/v) were added to maintain the culture pH of 8.0. Temperature and light were not controlled and reflected those naturally available in this area. The raceway ponds were inoculated with an inoculum/wastewater ratio of 240. At the time of harvesting, both ponds were colonized by microalgae consortiums of mainly green algae of the genera *Scenedesmus*, *Desmodesmus*, *Coelastrum* and *Chlorella*.

A microalgae paste was harvested once a week or every other week by sedimentation for about two days in 1 m³ plastic containers to pre-concentrate the microalgae, followed by centrifugation at ca. 5000 rpm (US Filtermaxx, Jacksonville, Florida, USA). For this study, a large amount of microalgae paste was needed, which was not possible to obtain from one harvest occasion. Therefore, the microalgae paste was harvested on twenty different dates between June and September from ponds 1 and 2 the samples were pooled. The pooled raw microalgae paste (MA) with 15% solids content was kept in the freezer at –20 °C until further use. MA was characterized to determine its carbohydrate, protein and ash contents, as described in the [Supplementary Information \(SI\)](#). The analysis showed it had 26.3 ± 8.59% carbohydrates, 26.9 ± 3.33% proteins and 16.4 ± 4.64% ash.

2.2. Experimental procedure

2.2.1. Lipid extraction of microalgae

The microalgae were subjected to a lipid extraction procedure adapted from the method optimized by Lage and Gentili [39], which originally consisted of a single-step method using a 2:1 chloroform:methanol (v/v) solution. In this study, the chloroform:methanol system was replaced by a DCM:hexane solution, which is less toxic and has higher extraction efficiency, as shown by Samburova et al. [40]. In brief, the frozen microalgae were slowly thawed overnight at room temperature, dried in an oven at 65 °C and ground into a fine powder. A volume of 300 mL of 1:1 DCM:hexane (v/v) solution was added to an Erlenmeyer flask containing 15 g of microalgae powder, and the mixture was vortexed for 15 min at ambient temperature. Cell debris was separated by vacuum filtration through a Whatman grade GF/C glass microfiber filter (1.2 µm) and rinsed with 300 mL of fresh 1:1 DCM:hexane (v/v) solution. The cake was dried until a constant weight at 65 °C and weighed to determine the dry solid weight. The dry solid consisting of the lipid-extracted microalgae biomass (EMA) was stored in a sealed plastic bucket until the subsequent carbonization experiments.

The extract was vacuum dried in a rotary evaporator (Rotavapor® R-300, Büchi Labortechnik AG, Switzerland) at 40 °C, 70 rpm and atmospheric pressure that was gradually decreased to 300 mbar to reduce the volume of solvents. The concentrated extract was transferred to a glass vial and dried in an oven at 65 °C until a constant weight to completely evaporate the solvents. Lastly, the lipid content per dry weight was gravimetrically determined. The lipids extracted represented 9.38 ± 0.23% of the microalgae polyculture biomass (dry basis, d.b.).

2.2.2. Hydrothermal carbonization experiments

HTC experiments were conducted in a 1 L stainless steel HTC reactor coupled with an internal water-cooling system (Amar Equipments Pvt. Ltd.). The feedstock was processed at 180, 210 and 240 °C for 1, 2 or 4 h. In the experiments conducted with raw microalgae paste (MA, with 15% solids), 650 g of MA was directly loaded into the reactor. In the experiments conducted with lipid-extracted microalgae (EMA), 88 g of EMA was mixed with 553 g of ultrapure water to adjust the extracted solid: water ratio to that of MA, then vortexed for 10 min and placed into the reactor. After the specific residence time, the reactor was cooled by the internal water-cooling system to room temperature and then depressurized by releasing the gaseous products to the fume extractor. The remaining slurry, consisting of the hydrochar and liquid fraction, was centrifuged at 4700 rpm for 20 min to separate the products. The hydrochar remaining in the centrifuge tubes was washed twice by adding 500 mL of ultrapure water, shaking vigorously for 5 min and centrifuging again to separate the washing water. The hydrochar was collected and placed in an oven at 65 °C until it was completely dried. Afterwards, it was weighed and finally ground and stored in a plastic sealed bucket prior to characterization and use. Samples were labeled as MA-T-t and EMA-T-t, where T refers to the carbonization temperature and t the residence time. We generated a set of 18 pristine hydrochar samples from the two different precursors at three temperatures and three residence times. Half of the material from each pristine hydrochar sample was subjected to the extraction procedure described in the following section to obtain a second set of samples consisting of washed hydrochars.

2.2.3. Extraction of hydrochars

Pristine hydrochars were extracted with DCM to separate the extractable fraction, which included secondary char and fatty acids, from the insoluble hydrochar structure attributed to the primary char. A volume of 20 mL of DCM per gram of dry hydrochar was mixed in an Erlenmeyer flask and vortexed for 30 min at ambient temperature. The solid was separated by vacuum filtration through a Whatman grade GF/C glass microfiber filter (1.2 µm) and rinsed with 8 mL of fresh DCM per gram of solid. The extract was concentrated in a rotary evaporator

Rotavapor® R-300 (Büchi Labortechnik AG, Switzerland) at 40 °C, 70 rpm and 1010 mbar. Concentrated extracts were transferred to a glass vial and dried in an oven at 65 °C until a constant weight to completely evaporate the solvent. Lastly, the extractive content of the hydrochars per dry weight was gravimetrically determined. The cake was dried until a constant weight at 65 °C and weighed to determine the dry solid weight. The dry solid, consisting of washed hydrochar, was stored in plastic sealed buckets prior to characterization. Samples were labeled as WMA-T-t and WEMA-T-t, where T refers to the carbonization temperature and t to residence time. Table S1 summarizes the set of samples produced in this work.

2.3. Analytical methods

2.3.1. Elemental composition

Elemental CHNS analysis of MA, EMA and the corresponding pristine and washed hydrochars was conducted in an Elemental CHNS Micro-analyzer Thermo Finningan Flash 1112 Series instrument. The analysis was carried out at the Research Technical Services of the University of Alicante (Alicante, Spain). Oxygen content was calculated by subtraction of the ash and CHNS content from the total.

2.3.2. Thermogravimetric analysis (TGA)

To investigate how HTC reaction conditions and the initial extraction of lipids from microalgae influence the formation and characteristics of primary and secondary char, TGA was performed for MA, EMA and the corresponding pristine and washed hydrochars. TGA is a powerful tool for analyzing changes in the hydrochar structure because it can provide valuable information on compositional changes, the formation and evolution of secondary and primary char and enable a wide range of HTC conditions to be studied based on the thermal stability of each fraction. TGA was conducted at the Research Technical Services of the University of Alicante (Alicante, Spain), using a Mettler Toledo TGA/DSC 2 Analyzer. The TGA method was based on the methodology developed by Saldarriaga et al. [41], which allows compositional changes to be studied as well as measurement of moisture, volatile matter (VM), fixed carbon (FC) and ashes in a single run. First, the sample was heated from 35 °C to 105 °C at 15 °C/min under a nitrogen atmosphere at 60 mL/min. Next, the temperature was held at 105 °C for 5 min to remove moisture. The sample was then heated from 105 to 700 °C at 15 °C/min and held at 700 °C for 30 min under the same nitrogen atmosphere to ensure the elimination of volatile matter. Finally, the atmosphere was switched to air at 60 mL/min while maintaining 700 °C for 5 min. During the last step, the fixed carbon was burnt and the final result was the ash content.

2.3.3. Pyrolysis-gas chromatography/mass spectrometry (Py-GC/MS)

Py-GC/MS analysis of MA, EMA and the corresponding pristine and washed hydrochars obtained at 240 °C for 4 h was conducted to identify substances released in each of the main decomposition stages identified in the TGA and to further understand changes in the hydrochar composition regarding primary char, secondary char and fatty acids. Pyrolysis experiments were conducted at 180, 275, 400 and 500 °C in an oven pyrolyzer equipped with an auto-sampler (PY-2020iD and AS-1020E, FrontierLabs, Japan) connected to a GC/MS system (Agilent, 7890A-5975C, Agilent Technologies AB, Sweden). The Py-GC/MS conditions were as suggested by Tolu et al. [42]. In brief, the Py/GC interface and GC injector temperatures were set to 320 °C. The injector was operated with helium as the carrier gas and a split ratio of 16:1. After one minute, the gas-saver mode was used with a flow rate of 50 mL min⁻¹ to vent the pyrolysate bleed of the sample remaining in the pyrolyzer oven. The GC temperature program increased the temperature from 40 °C to 320 °C at a rate of 10 °C min⁻¹ and the last temperature was held for 7 min. The pyrolysate was separated on a DB-5MS capillary column (30 m, 0.25 mm i.d., 0.25 µm film thickness; J&W, Agilent Technologies AB, Sweden). The GC/MS interface was kept at 280 °C.

The mass spectrometer with a quadrupole type analyzer was operated at unit mass resolution and scanned over the mass range m/z 35 to 500 at 3.1 scan s⁻¹. For ionization, 70 eV electron bombardment was used. Volatile substances desorbed from the materials were mainly expected at 180 and 275 °C, whereas at higher pyrolysis temperatures, decomposition products were expected as well. All the organic compounds were considered as target compounds. Therefore, the Py-GC/MS analysis provided an extensive dataset that was systematically analyzed to extract as much information as possible. Qualitative peak identification was conducted by comparing the collected ion spectra to reference mass spectral libraries (NIST08 and WILEY7n). An 80% level of certainty in the spectral match criteria was used as a cut-off for spectral identification.

3. Results and discussion

3.1. HTC performance

Hydrochar yields from a raw microalgae polyculture (MA) and extracted microalgae polyculture (EMA) at different temperatures and residence times are shown in Fig. 2. Solid yields were in the range 38–55 % and showed an inverse covariation with increasing reaction temperature and residence time due to the combined effect of increased polymerization and formation of secondary char along with the decomposition of microalgae biomass to liquid/gaseous products. The solid yields in this study were lower than those obtained from HTC processing of lignocellulosic biomass, which ranged from 50 to 80% under similar reaction conditions [6,26,43]. Similar results were also found by Ekpo and co-authors [19], who observed hydrochar yields from *Chlorella vulgaris* as low as 35% at 250 °C for 1 h, nearly 2 times lower than hydrochar yields from digestate and swine manure under the same conditions. Extraction of lipids from microalgae generally resulted in slightly lower hydrochar yields, in agreement with the literature [17,20,21]. Broch et al. [17] found that the solid yield from *C. vulgaris* carbonized at 175 °C and 1 h decreased from 49.3% to 44.6% when the microalgae were extracted with DCM prior to HTC. Likewise, comparisons between the works conducted by Lee et al. [20] and Park et al. [21] showed that solvent extraction of microalgae prior to HTC reduced the solid yield from *C. vulgaris* from 59.0 to 51.8% even at shorter reaction times under the same HTC temperature.

The increase in severity of reaction conditions had different effects on the development of the extractable and non-extractable matter during HTC under the range of operational parameters studied (Fig. 2). Increasing the temperature and residence time promotes biomass degradation to dissolved fragments in the liquid phase and polyaromatic non-extractable char [34,43]. As the reaction progresses, liquid products polymerize and condense on the primary char, forming the secondary char. Thus, as a result of the solid degradation and secondary char formation, the contribution of the non-extractable hydrochar to the global solid yield decreased with increasing temperature and residence time, whereas the contribution of the extractable matter to the hydrochar yield increased.

3.2. Composition of the hydrochars

The proximate and elemental composition of MA, EMA and hydrochars are shown in Table 1. In general, the composition of the hydrochars varied only slightly with residence time and somewhat more with temperature. The carbon content ranged from 47.65 to 52.07% for the MA-derived hydrochars and 44.80 to 46.47 for EMA-derived hydrochars. Likewise, increasing the temperature from 180 to 240 °C only resulted in a slight variation of 5% and 2% in VM and FC, respectively, values that slightly increased to 17% and 10% when MA was subjected to lipid extraction prior to the HTC process. More remarkable though were the compositional changes observed for the hydrochars in comparison with their respective feedstocks. VM decreased by 23%, FC

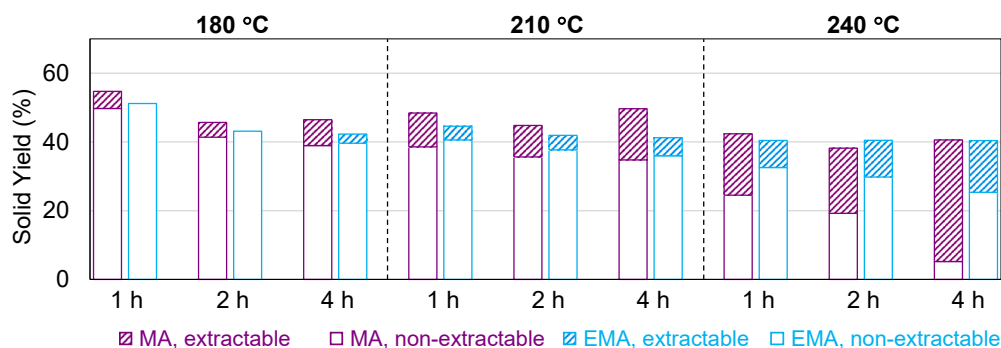


Fig. 2. Hydrochar yields from an unextracted (MA) and extracted (EMA) microalgae polyculture at different temperatures and residence times. The hatched area represents the solid yield corresponding to extractable matter and the white area to non-extractable matter. The sum of hatched and white areas represents the total solid yield.

Table 1

Influence of temperature and residence time on the composition of hydrochars produced from an unextracted (MA) and extracted (EMA) microalgae polyculture.

Sample ID	% (dry basis)								H/C	O/C
	VM	FC	Ash	C	H	N	S	O		
MA	70.48	13.72	15.81	44.21	6.54	6.95	0.36	26.13	1.77	0.44
EMA	68.92	14.47	16.61	44.58	6.11	7.45	0.33	24.93	1.65	0.42
MA-180-1	57.34	17.05	25.61	47.65	5.72	4.86	0.14	16.02	1.44	0.25
MA-180-2	58.17	15.61	26.22	47.69	5.59	4.43	n.d.	16.07	1.41	0.25
MA-180-4	56.56	16.20	27.24	47.94	6.06	4.24	0.14	14.37	1.52	0.22
MA-210-1	55.47	17.09	27.44	48.80	5.97	4.02	0.22	13.55	1.47	0.21
MA-210-2	54.06	17.24	28.70	48.73	5.96	4.02	0.16	12.44	1.47	0.19
MA-210-4	54.26	16.68	29.06	49.12	6.19	4.07	n.d.	11.56	1.51	0.18
MA-240-1	52.96	17.50	29.54	50.81	6.07	4.10	0.21	9.27	1.43	0.14
MA-240-2	53.33	17.31	29.35	51.74	5.75	4.22	n.d.	8.93	1.33	0.13
MA-240-4	54.26	16.68	29.06	52.07	6.38	4.06	n.d.	8.43	1.47	0.12
WMA-180-1	57.63	15.63	26.73	42.55	5.17	4.84	n.d.	20.71	1.46	0.37
WMA-180-2	54.77	16.01	29.21	44.92	5.40	4.69	n.d.	15.79	1.44	0.26
WMA-180-4	51.42	17.16	31.42	43.13	5.04	4.56	n.d.	15.86	1.40	0.28
WMA-210-1	47.79	17.68	34.52	42.65	4.84	4.09	n.d.	13.90	1.36	0.24
WMA-210-2	46.40	17.78	35.82	43.39	4.91	4.27	n.d.	11.61	1.36	0.20
WMA-210-4	41.88	18.86	39.26	41.43	4.71	4.16	n.d.	10.43	1.36	0.19
WMA-240-1	41.49	18.13	40.39	41.51	4.46	3.99	n.d.	9.65	1.29	0.17
WMA-240-2	39.85	16.10	44.04	40.85	4.34	3.89	n.d.	6.87	1.28	0.13
WMA-240-4	33.13	13.07	53.80	31.71	3.46	3.09	n.d.	7.94	1.31	0.19
EMA-180-1	59.55	14.48	25.97	44.80	5.63	5.39	0.10	18.11	1.51	0.30
EMA-180-2	57.48	15.34	27.17	44.12	5.50	4.79	n.d.	18.41	1.50	0.31
EMA-180-4	57.07	14.87	28.06	44.77	5.48	4.41	n.d.	17.28	1.47	0.29
EMA-210-1	54.73	14.94	30.33	44.67	5.42	4.13	n.d.	15.44	1.46	0.26
EMA-210-2	51.55	16.23	32.22	44.37	5.07	3.92	n.d.	14.43	1.37	0.24
EMA-210-4	50.67	15.77	33.56	45.00	5.21	3.78	n.d.	12.45	1.39	0.21
EMA-240-1	49.36	16.01	34.63	44.64	5.17	3.73	0.16	11.67	1.39	0.20
EMA-240-2	49.69	15.33	34.98	46.29	5.26	3.95	n.d.	9.52	1.36	0.15
EMA-240-4	49.47	15.93	34.61	46.47	5.10	4.01	n.d.	9.81	1.32	0.16
WEMA-180-1	58.09	14.80	27.10	41.79	5.20	5.57	n.d.	20.33	1.49	0.36
WEMA-180-2	56.93	14.48	28.59	42.24	5.21	5.14	n.d.	18.81	1.48	0.33
WEMA-180-4	54.42	15.54	30.04	41.79	5.14	4.57	n.d.	18.46	1.48	0.33
WEMA-210-1	51.09	15.46	33.46	40.80	4.91	4.23	n.d.	16.61	1.44	0.31
WEMA-210-2	49.30	16.42	34.28	42.29	4.68	4.01	n.d.	14.74	1.33	0.26
WEMA-210-4	46.43	15.78	37.78	40.94	4.69	3.76	n.d.	12.83	1.38	0.24
WEMA-240-1	42.61	15.96	41.44	39.02	4.45	3.50	0.24	11.36	1.37	0.22
WEMA-240-2	41.00	15.31	43.68	38.26	4.26	3.55	n.d.	10.25	1.34	0.20
WEMA-240-4	38.44	15.77	45.79	36.95	3.94	3.54	n.d.	9.77	1.28	0.20

increased by 22% and the C content increased by 18% at the highest HTC temperature and residence time tested in comparison to the raw microalgae. For the lipid-extracted microalgae biomass, the variation in FC and C content was only 10% and 4%, respectively. Regarding VM, the hydrochar exhibited a 9% lower volatile content when the feedstock was subjected to lipid extraction.

The hydrochars had lower amounts of N compared with MA and EMA. Between 58 and 70% of the N contained in the feedstock was retained in the MA-derived hydrochars, with the rest released as aqueous species, as described previously in the literature [14,44].

Similar retention efficiencies of N were found for EMA-derived hydrochars. With increasing temperature and residence time, a decrease of N content was observed, which was likely a consequence of an increased hydrolysis rate of proteins and amino acids to soluble organic compounds and ammonium salts at higher temperatures [44]. At 240 °C, a small increase at long residence time was exhibited, perhaps due to the precipitation of inorganic nitrogen compounds, e.g., nitrates/nitrites, but also the extended incorporation of nitrogen-containing compounds into the hydrochar via, e.g., a type of Maillard reaction [44]. The N content was lower in the washed hydrochars than their pristine

counterparts, which may indicate the formation of extractable N-compounds during HTC at 240 °C and their subsequent removal during the washing. When pristine hydrochars were washed with DCM, their composition was dramatically affected (Table 1), especially for hydrochars generated under the most severe HTC conditions, indicating that the high temperature hydrochars were very rich in extractable matter.

Extractives resulting from the HTC process were first found at 180 °C after the process had been maintained for 4 h, as demonstrated by the results obtained for EMA-derived hydrochars (Fig. 3). Until 210 °C and 2 h residence time, differences in the extractive content between the MA- and EMA-derived hydrochars were attributed to the lipids extracted from MA, since the extractive content of MA-derived hydrochars could be described as the sum of the extractives generated in HTC, i.e., extractive content of EMA-derived hydrochars, plus the initial extractive content of MA. However, differences between the extractive content of MA and EMA-derived hydrochars increased as the HTC processing severity increased. This suggests that MA degraded to a greater extent than EMA and led to increased formation of secondary char under the same HTC conditions. Moreover, more decomposition products may have remained solubilized in the liquid phase and less polymerization and deposition of secondary char may have occurred during the carbonization of lipid-extracted microalgae, which would explain the lower solid yield resulting from the carbonization of EMA in comparison to MA. In agreement with this observation, the carbonization extent of MA was found to be higher than that of EMA under the same temperature and residence time conditions in HTC. Results obtained for WMA-hydrochars and WEMA-hydrochars showed that MA underwent greater conversion than EMA under the same temperature and time conditions (Fig. 4), mainly via a hydrolysis reaction pathway, as first suggested by Heilmann et al. [12]. This further demonstrates the effect of lipid extraction of the microalgae polyculture prior to HTC on the carbonization process.

3.3. Formation and characteristics of primary and secondary char by TGA and Py-GC/MS

Supporting results were obtained from TGA, which also revealed differences in hydrochar composition depending on whether or not lipid extraction of MA had been conducted prior to HTC. The rate of material weight loss (DTG, expressed as %/°C) against temperature is plotted in Fig. 5 for feedstocks MA and EMA, pristine hydrochars MA-240-4 and EMA-240-4, and the corresponding washed hydrochars WMA-240-4 and WEMA-240-4. Only the DTG curves for hydrochars produced at 240 °C for 4 h are presented in Fig. 5 since changes induced under milder HTC

conditions followed the same trends and were proportional to the HTC severity. For this reason, only Py-GC/MS analysis of hydrochars produced at 240 °C and 4 h were conducted to identify the maximum number of compounds. Additional DTG curves can be found in Figs. S2 to S9 (SI).

DTG curves were divided into four stages corresponding to the most significant mass losses: a devolatilization stage (stage 1, less than 200 °C), low temperature shoulder (stage 2, 200–300 °C), sharp peak (stage 3, 300–400 °C) and high temperature shoulder (stage 4, >400 °C). Stage 1 corresponded to dehydration of cellular and external moisture along with desorption of highly volatile substances. In this stage, the cell structure is destroyed with alteration of lipid structures and protein thermal unfolding [46]. Stages 2 and 3 were associated with the decomposition of proteins and carbohydrates [46]. Stage 2 might also have included desorption of high molecular weight substances. Stage 4 corresponded to degradation of higher-weight compounds. Mass losses corresponding to MA and EMA in stages 1 to 3 were shifted toward higher temperatures after the HTC processing of the feedstocks, indicating that the hydrochars were more thermally stable than the feedstocks. A comprehensive analysis of the events occurring in each stage was conducted to understand possible changes in secondary and primary char and their modification following lipid extraction from microalgae prior to HTC processing.

Stage 1 (<200 °C): Compounds extracted during the lipid extraction of MA appeared mainly devolatilized below 200 °C in the TGA because no significant differences were observed between MA and EMA in the following stages. The MA and EMA data from Py-GC/MS analysis at 180 °C, under which only the desorption of substances could take place, showed that the main compounds removed or partially removed by lipid extraction were 9-hexadecanoic acid, docosane, 1-tricosanol and cholestan-3-ol. Py-GC/MS at 275 °C showed the desorption of higher molecular weight byproducts of lipids only partially removed during the lipid extraction of MA (e.g., verbenol, *n*-hexadecanoic acid, oleic acid, 2-myristinoyl pantetheine, campesterol and cholesterol), which were removed from MA in a percentage higher than 50%. For hydrochars, the first devolatilization stage was extended to 240 °C. Desorbed compounds identified from Py-GC/MS of MA and EMA were also identified in the Py-GC/MS analysis of MA and EMA-derived hydrochars, but the TIC/mg of these substances exceeded the corresponding amounts found in MA and EMA. In addition, a wider range of devolatilized substances from hydrochars was found by Py-GC/MS at 180 °C and 275 °C, including fatty acid byproducts (e.g., 1-tricosanol, stigmaterol, 1-docosanol, isochiapin B, stigmasta-5,22-dien-3-ol) and nitrogenated compounds (e.g., *N,N*-dimethyldodecanamide, *N,N*-diethyldodecanamide,

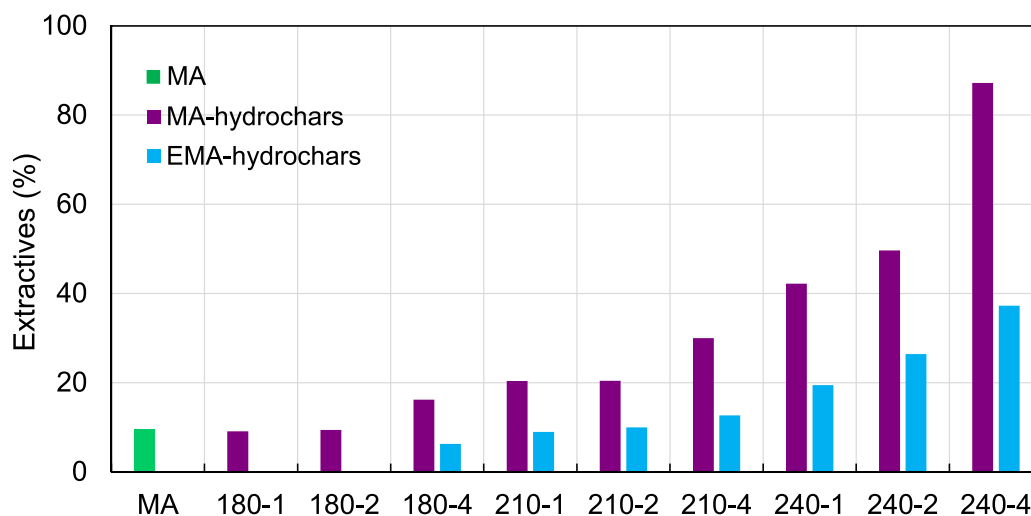


Fig. 3. Extractive content of hydrochars produced from an unextracted (MA) and extracted (EMA) microalgae polyculture.

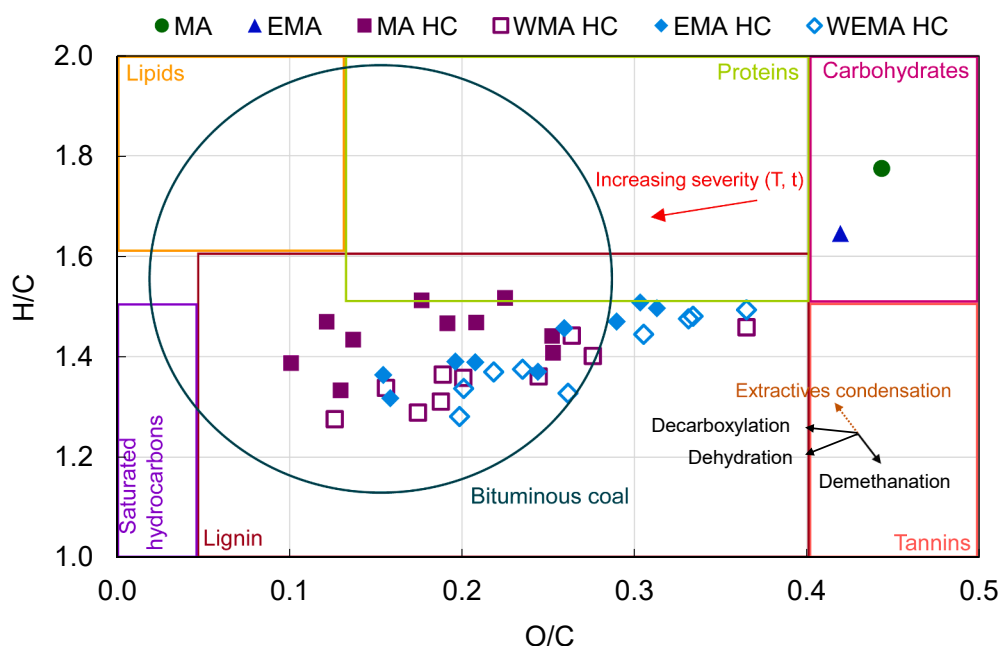


Fig. 4. Van Krevelen diagram representing feedstocks and hydrochars produced from an unextracted (MA) and extracted (EMA) microalgae polyculture (background of the figure adapted from [45]).

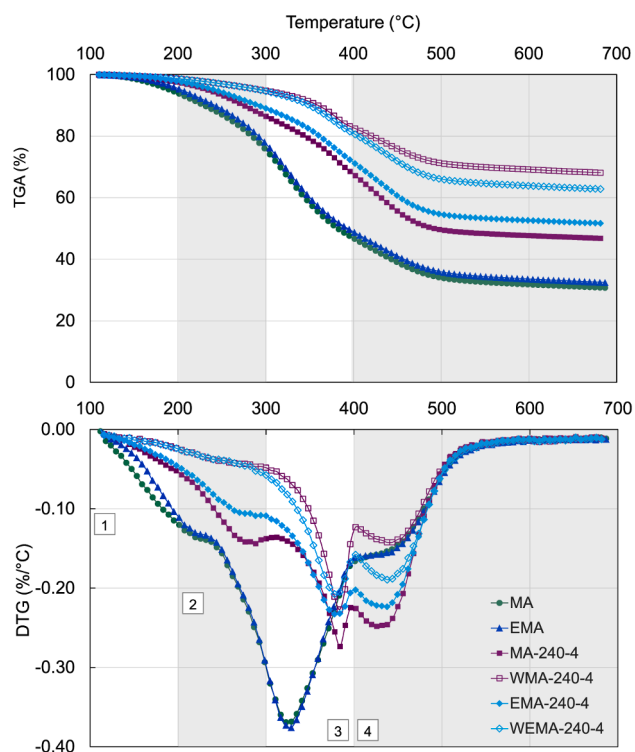


Fig. 5. TGA and DTG curves of feedstocks MA and EMA and corresponding pristine and washed hydrochars produced at 240 °C for 4 h.

1-(1-oxooctadecyl)-pyrrolidine and colchifoleine, *N*-butyl-9-octadecanamide and oleic diethanolamide). These compounds were all extractable after HTC as they were not among the substances identified in the Py-GC/MS analysis of washed hydrochars. Thus, the results suggested that the fatty acid byproducts were more susceptible to being extracted after HTC in comparison to MA. Hence, HTC treatment of MA promoted

the extractive removal efficiency. This finding is valuable since it suggests that HTC may be a useful pretreatment for MA for subsequent lipid extraction, e.g., for biofuel production, although this is not the scope of this study.

Stage 2 (200–300 °C): The shoulder centered at 240 °C for MA and EMA was shifted to 285 °C for the corresponding pristine and washed hydrochars (Fig. 5). The total mass loss (%) associated with stages 1 and 2 (Table 2) was comparable for MA and MA-240-4. However, the extractable matter substantially increased after HTC in detriment to the non-extractable fraction because the mass loss (%) corresponding to WMA-240-4 was reduced by 60.8% (Table 2). Py-GC/MS analysis at 275 °C showed that light compounds found in MA were either not detected in MA-240-4 or detected in significantly lower amounts (TIC/mg reduced by > 80%). On the other hand, the analysis showed that a variety of new compounds with high molecular weight were formed during HTC. Thus, the TIC/mg of, e.g., pentanoic acid, 2-2-cyclohexylpiperidine, 9-eicosene and phytol was decreased by > 85%, whereas acetic acid, alanine, glycerine, 2-pyrrolidinone and uric acid, among others, were not detected in the pristine hydrochar sample, indicating that the precursors were transformed during HTC. Likewise, significant increases in nitrogenated compounds (e.g., trimethylamine, hexadecanamide, 9-octadecanamide) and fatty acid byproducts (e.g., 2-hexadecane, cyclotetracosane, stigmaterol) were detected in hydrochars, suggesting that these substances resulted from new phases/compounds formed during HTC that degraded in stage 2 (Fig. 5). The cumulative mass loss (%) found for EMA-240-4 was slightly lower than for MA-240-4 in the

Table 2

Cumulative mass loss (%) of an unextracted (MA) and extracted (EMA) microalgae polyculture, and corresponding pristine and washed hydrochars produced at 240 °C for 4 h.

Total mass loss (%)	MA	EMA	MA-240-4	EMA-240-4	WMA-240-4	WEMA-240-4
Stage 1	-4.76	-3.34	-1.81	-1.58	-0.99	-1.03
Stage 2	-11.58	-9.79	-11.47	-9.31	-4.50	-4.58
Stage 3	-53.36	-51.24	-31.47	-27.65	-16.77	-18.47
Stage 4	-70.40	-68.84	-54.19	-49.39	-33.03	-38.34

same temperature region (Table 2). Accordingly, the TIC/mg of the substances detected in the Py-GC/MS analysis of EMA-240-4 was generally lower than the corresponding TIC/mg of the same substances released from MA-240-4. Nevertheless, the reduction of TIC/mg between feedstocks and associated pristine hydrochars was comparable for MA and EMA (Table 2), suggesting that MA- and EMA-components degraded in TGA stage 2 underwent the same degree of conversion during HTC. The overlapping of the WMA-240-4 and WEMA-240-4 curves in stages 1 and 2 supports this hypothesis, as it indicates that washed hydrochars (primary char) exhibit the same thermal stability, and therefore underwent the same conversion rate during HTC. This may have led to MA- and EMA-components degraded in TGA stage 2 reacting during HTC to form more thermally stable substances and/or compounds retained in the HTC liquor and subsequently recondensed on the solid surface in the form of extractable high molecular weight substances. During HTC of MA, more re-polymerization and recondensation over the solid surface was observed in comparison to EMA, forming more secondary char that in turn led to a higher extractive content (stage 2, Fig. 5), further supporting the discussion in section 3.2. However, for both MA and EMA, some substances increased substantially after HTC. For instance, the TIC/mg of fatty acids, such as oleic acid, cholest-4-ene, cholesterol and campesterol, increased by > 75% for pristine hydrochars in comparison to their corresponding feedstocks. This finding indicates, as observed in stage 1, that these fatty acids released from microalgae structures degraded during HTC became more accessible during the subsequent extraction of the hydrochars.

Stage 3 (300–400 °C): The mass loss (%) associated with MA and EMA in stage 3 was substantially decreased for the corresponding pristine and washed hydrochars (Table 2). Accordingly, an increase in mass loss in stage 4 was observed for hydrochars in comparison to their respective feedstocks, although the increase did not entirely correspond to the decrease in mass loss observed in stage 3. These results indicate that: (i) MA components degraded in stage 3 were not extracted during the lipid extraction of MA because the DTG curves for MA and EMA overlapped in stage 3; (ii) during HTC, these MA components (also contained in EMA) were potentially transformed into more thermally stable products (e.g., degradable in stage 4 or at even higher temperatures), which could include extractable and non-extractable substances; (iii) these transformations may also have led to secondary products that were transferred to the HTC liquor and/or gas phase; (iv) some of these MA components may have been directly converted into products that were transferred to the HTC liquor and/or gas phase; (v) some of the products transferred to the HTC liquor may have subsequently polymerized and condensed over the solid in the form of high weight extractives (i.e., secondary char, heavier than that desorbed/degraded in stage 2), which might have induced the mass gain in stage 4; and (vi) the transfer of substances to the HTC liquor and/or gas phase may explain the differences observed between the mass lost in stage 3 (41 %wt) and the mass gained in stage 4 (6 %wt). Stage 3 was associated with the decomposition of proteins and carbohydrates [46], which agrees well with the Py-GC/MS results at 400 °C showing that the main degradation products from MA, EMA and the corresponding hydrochars were proteins (i.e., nitrogenated compounds) and carbohydrate derivatives (i.e., glucopyran, pyranes, aliphatic and ketones). As expected, the TIC/mg of low molecular weight byproducts from proteins and carbohydrates found for MA and EMA was substantially decreased after HTC due to reactions during the HTC processing and subsequent solubilization in the liquid phase. The dissolved products may have further polymerized and precipitated on the primary char surface, forming secondary char. As a result, a variety of high molecular weight pyrolysis byproducts were detected in the Py-GC/MS analysis at 400 °C of the pristine hydrochars. Among them, protein derivatives were formed to a lesser extent than carbohydrate derivatives, which is consistent with the literature [31,44]. Fatty acid decomposition products were also found (aldehydes, aliphatic compounds, alcohols, carboxylic acids and esters) among the substances released during the thermal treatment of MA, EMA and their

corresponding pristine hydrochars at 400 °C. Low molecular weight byproducts released during the pyrolysis of MA and EMA were decreased after HTC, whereas high molecular weight pyrolysis byproducts increased during the pyrolysis of pristine hydrochars at 400 °C.

Stage 4 (>400 °C): The WMA-240-4 sample formed the basis for understanding potential changes occurring during HTC. The difference in mass loss (%) between WMA-240-4 (and feedstocks) and MA-240-4 (6 %wt) was interpreted as mass associated with extractives formed during HTC degrading in stage 3. The mass gain of EMA hydrochars in comparison to WMA-240-4 was attributed to the remaining non-extractable phases (4 %wt) and the formation of new extractable phases (2 %wt). Differences between WMA-240-4 and WEMA-240-4 indicated structural and/or compositional differences between the non-extractable phases of the corresponding hydrochars. The higher mass loss of WEMA-240-4 in comparison to WMA-240-4 indicated that non-extractable compounds contained in EMA-240-4 were less thermally stable than the non-extractable fraction forming MA-240-4. In addition, the difference in mass loss between WMA-240-4 and WEMA-240-4 corresponded to the amount of extractable matter in MA-240-4, and this mass loss was not exhibited by MA or EMA. This result suggests that the difference in mass loss between WMA-240-4 and WEMA-240-4 corresponded to non-extractable intermediate products. As a result, less secondary char was formed and deposited on the primary char surface, and therefore less extractable matter was found in the TGA (Fig. 5). Consequently, we concluded that the EMA-derived hydrochars had a lower carbonization degree than the MA-derived hydrochars, in agreement with the Van Krevelen diagram (Fig. 4). Supporting results were found in the Py-GC/MS analysis conducted at 500 °C. The MA and EMA-derived hydrochars differed in their pyrolysis byproduct profile, indicating that lipid extraction of MA altered the non-extractable fraction. A complete list of the main compounds identified by Py-GC/MS (Table S2) shows that during HTC of MA, the TIC/mg of some compounds increased (e.g., methylcyclopentane, pyridine, uric acid, 5,8-diethyldodecane, 9-eicosane, 9-octadecenamamide), whereas the TIC/mg of other substances decreased dramatically in comparison to EMA (e.g., acetaldehyde, nonanal, octanal, 4-propyl-heptane, azido-cyclohexane, which in general have lower molecular weight and therefore are associated with less carbonized components).

To sum up, the lipid extraction of MA hindered the carbonization of the material and resulted in hydrochars with less severely carbonized primary char and a lower amount of secondary char deposited on its surface. This raises questions about how lipid extraction prior to HTC affects the composition of the secondary char and what, if any, phytotoxic properties this may induce. This is a matter of high concern for several hydrochar applications, mainly those related to agricultural practices.

3.4. Evaluation of hydrochar phytotoxicity by Py-GC/MS

Previous investigations have revealed that several volatile and semi-volatile organic compounds in pristine hydrochars might be associated with toxic effects [47,48]. Potentially toxic substance groups are organic acids, aldehydes, ketones and furans, benzene and its derivatives, and phenolic compounds. Phenolic compounds along with organic acids, ketones and furans are known to be microbial and seed germination inhibitors [49,50], nematicidal toxicants [51], and especially for polyphenols, have been observed to shift the dominant pathway of N-cycling from mineral to organic N-forms [52–54]. Similarly, benzene and its derivatives have been reported to display eco-toxicological effects even in the ppm range [55]. The toxicity may depend on the compound concentration as well as matrix interactions, although these interactions remain unknown [10]. Whatever their degree of phytotoxicity, most potentially toxic compounds contained in the hydrochars are volatile at temperatures up to 200–300 °C [56], and therefore their presence in MA and EMA hydrochars was estimated using Py-GC/MS analysis at 180 °C.

Initially, Py-GC/MS analysis at 275 °C was considered as well, but additional compounds in this analysis compared to at 180 °C only represented 1.3–9.5% of the total peak area and were mainly attributed to pyrolysis degradation products. Therefore, only data obtained at 180 °C were considered with regard to potentially toxic compounds. Although Py-GC/MS is a qualitative technique, the total peak area and TIC/mg of potentially toxic substance groups (Fig. 6, Figs. S10 to S12, Table S3) may still be useful indicators to estimate the total phytotoxicity of the hydrochars since differences in peak height between chromatograms may be proportional to the concentrations [57].

Assessing the amounts of potentially toxic substances groups released from MA, EMA and the corresponding pristine and washed

hydrochars showed that carboxylic acids represented almost half of the total substances released from MA and EMA (Fig. 6). The contribution of carboxylic acids decreased to 20.9 and 23.1% for MA and EMA-derived hydrochars, respectively. Moreover, they were associated with the lipids contained in the feedstocks and retained on the hydrochar surface. Lipid extraction of the microalgae prior to HTC was observed to reduce the formation of potentially toxic substances in the secondary char. The TIC/mg of aldehydes and ketones from EMA hydrochars was 41 and 43% lower, respectively, than the TIC/mg associated with MA-hydrochars, while phenolics, benzene and its derivatives were not detected. Therefore, in addition to affecting the carboxylic acid content of the extractable matter, extraction of lipids of MA prior to HTC had an

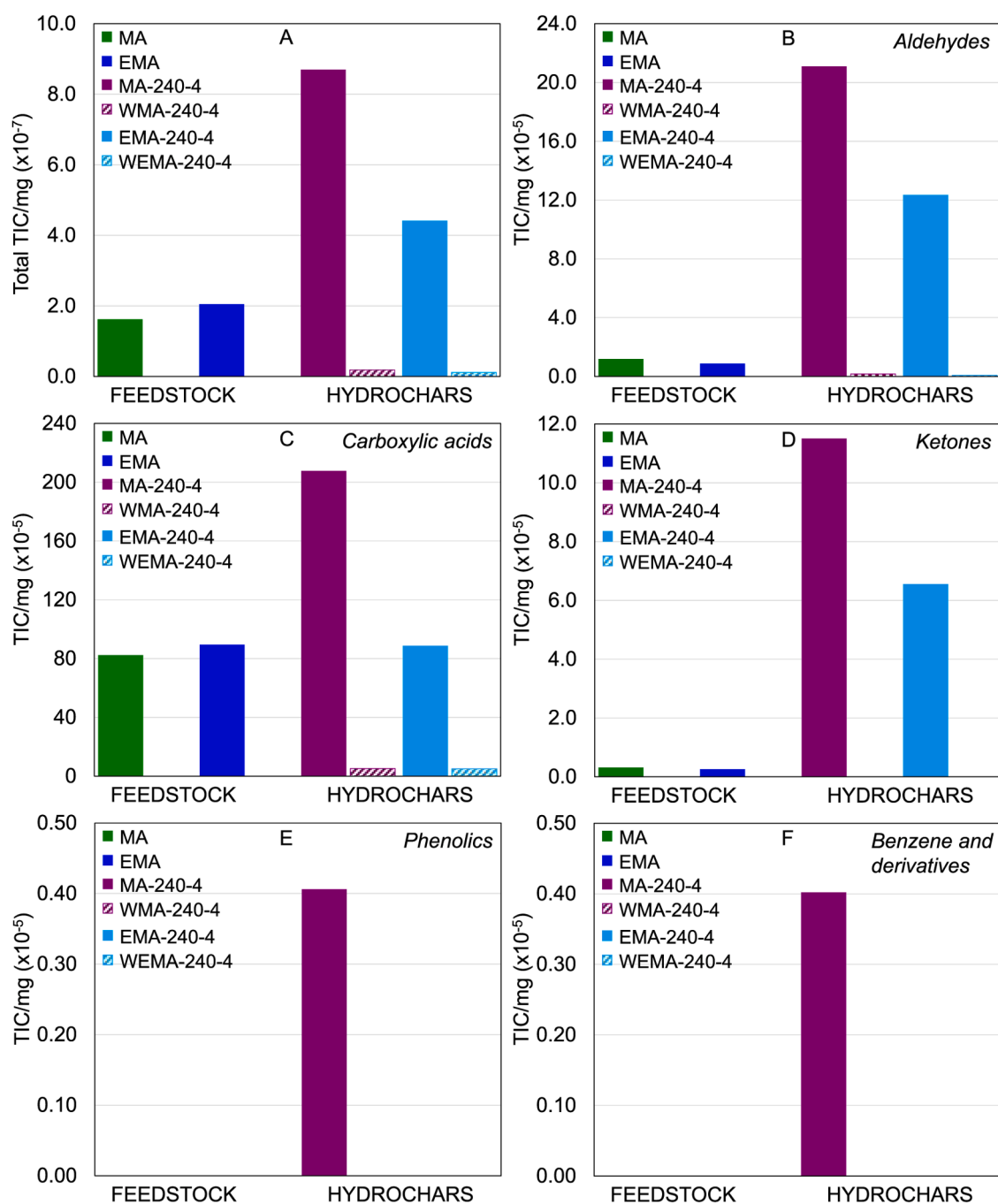


Fig. 6. Total amount of organic compounds and relative amounts of potentially toxic substances released during Py-GC/MS analysis at 180 °C of hydrochars produced at 240 °C and 4 h from an unextracted (MA) and extracted (EMA) microalgae polyculture. (a) Total TIC/mg, (b) TIC/mg of aldehydes, (c) TIC/mg of ketones (d) TIC/mg of carboxylic acids, (e) TIC/mg of phenolics, (f) TIC/mg of benzene and its derivatives.

impact on the carbonization of the material, composition of the extractable fraction of the hydrochar and, ultimately, its phytotoxic potential.

Despite the initial lipid extraction and its effect on the composition of the secondary char, carboxylic acids represented the main source of phytotoxic compounds. Therefore, depending on the intended application of the hydrochar, it may be necessary to remove these prior to use, e.g., as a soil amendment. This can be achieved either by improving the efficiency of the lipid extraction prior to HTC or by post-treatment of the hydrochar product. Likewise, the elimination of other phytotoxic substances in the hydrochar may be required. Fig. 6 and Figs. S10 to S12 shows that, unsurprisingly, washing of the hydrochars with DCM effectively removed > 97% of the organic substances found in MA and EMA-derived hydrochars. However, this approach generates a secondary residue that would mean loss of C unless directed to, e.g., biodiesel production. To maximize the benefit of the carbon sequestration gained during the microalgae growth, other possible and higher value uses for the microalgae-derived hydrochars would be more desirable. Hydrochar extractives contained hydrophobic (fatty acids) and hydrophilic (e.g., aldehydes and ketones) functional groups may enable hydrochars to be used as adsorbents for environmental remediation or as reinforcing additives in composite materials. Further investigations on applications in these and related areas will be critical for the continued development of carbon negative applications based on microalgae-derived hydrochars.

4. Conclusions

The obtained results showed that lipid extraction of a microalgae polyculture prior to HTC processing had a pronounced impact on the carbonization of the material, chemical composition of the extractable hydrochar and, ultimately, its phytotoxic potential. Unextracted microalgae exhibited a greater carbonization degree than lipid-extracted microalgae and generated a hydrochar with higher amounts of secondary char than the corresponding EMA hydrochar under the same HTC conditions. The results also indicated that the carbonization of lipid-extracted microalgae resulted in more liquid products and less polymerization and formation of secondary char, which would explain the lower solid yield resulting from the carbonization of lipid-extracted microalgae in comparison to unextracted microalgae and the reduced amount of substances that might be responsible for the phytotoxic properties of the hydrochar.

Despite the reduced hydrochar phytotoxicity induced by lipid extraction, high temperature hydrochars contained significant amounts of potentially toxic substances. To use these hydrochars in applications involving microorganisms and plant cultivation, toxic substances present should be removed, which could potentially have a negative impact on the efficiency of the whole system as a carbon capture technology. Therefore, while low-temperature hydrochars containing less than 10% of extractives might serve as a plant cultivation media, extractive-rich hydrochars would be more convenient for other long-term applications by functioning as carbon sinks, such as adsorbents for contaminant removal, energy storage and reinforcing additives in composite materials. Further studies are needed to investigate complementary physicochemical properties of microalgae-derived hydrochars in order to match these materials with preferred utilization areas.

Declaration of Competing Interest

The authors declare that they have no known competing financial interests or personal relationships that could have appeared to influence the work reported in this paper.

Acknowledgments

The authors acknowledge Bio4Energy (www.bio4energy.se), a

strategic research environment appointed by the Swedish government, for supporting this work. We thank Annika Holmgren (Department of Wildlife, Fish, and Environmental Studies, Swedish University of Agricultural Sciences) for assistance in microalgae harvesting. The Swedish Metabolomics Centre, Umeå, Sweden is acknowledged for amino acid quantification by LC-MSMS. The help of technical staff at Vakin AB, Umeå Energi AB and Ragnsells AB is greatly appreciated.

Funding: This work was supported by The Swedish Research Council for Environment, Agricultural Sciences and Spatial Planning (Formas) under grants no 2018-00532 and 942-2015-92, Vinnova (project nr. 2017-03301), EU Interreg Botnia-Atlantica (TransAlgae project), and the Kempe Foundation.

Appendix A. Supplementary data

Supplementary data to this article can be found online at <https://doi.org/10.1016/j.cej.2021.129559>.

References

- [1] J.K. Pittman, A.P. Dean, O. Osundeke, The potential of sustainable algal biofuel production using wastewater resources, *Bioresour. Technol.* 102 (2011) 17–25, <https://doi.org/10.1016/j.biortech.2010.06.035>.
- [2] B. Wang, Y. Li, N. Wu, C.Q. Lan, CO₂ bio-mitigation using microalgae, *Appl. Microbiol. Biotechnol.* 79 (2008) 707–718, <https://doi.org/10.1007/s00253-008-1518-y>.
- [3] S. Lage, Z. Gokjovic, C. Funk, F.G. Gentili, Algal biomass from wastewater and flue gases as a source of bioenergy, *Energies* 11 (2018) 664, <https://doi.org/10.3390/en11030664>.
- [4] A. Yamasaki, An overview of CO₂ mitigation options for global warming-Emphasizing CO₂ sequestration options, *J. Chem. Eng. Japan* 36 (2003) 361–375, <https://doi.org/10.1252/jcej.36.361>.
- [5] C. Stewart, M.A. Hessami, A study of methods of carbon dioxide capture and sequestration-the sustainability of a photosynthetic bioreactor approach, *Energy Convers. Manag.* 46 (2005) 403–420, <https://doi.org/10.1016/j.enconman.2004.03.009>.
- [6] J.A. Libra, K.S. Ro, C. Kammann, A. Funke, N.D. Berge, Y. Neubauer, M.M. Titirici, C. Fühner, O. Bens, J.K.K.H. Emmerich, Hydrothermal carbonization of biomass residuals: a comparative review of the chemistry, processes and applications of wet and dry pyrolysis, *Biofuels* 2 (2011) 89–124, <https://doi.org/10.4155/bfs.10.81>.
- [7] M.M. Titirici, R.J. White, C. Falco, M. Sevilla, Black perspectives for a green future: hydrothermal carbons for environment protection and energy storage, *Energy Environ. Sci.* 5 (2012) 6796–6822, <https://doi.org/10.1039/C2EE21166A>.
- [8] J.F.R. Flora, X. Lu, L. Li, J.R.V. Flora, N.D. Berge, The effects of alkalinity and acidity of process water and hydrochar washing on the adsorption of atrazine on hydrothermally produced hydrochar, *Chemosphere* 93 (2013) 1989–1996, <https://doi.org/10.1016/j.chemosphere.2013.07.018>.
- [9] N.D. Berge, K.S. Ro, J. Mao, J.R.V. Flora, Hydrothermal carbonization of municipal waste streams, *Environ. Sci. Technol.* 45 (2011) 5696–5703, <https://doi.org/10.1021/es2004528>.
- [10] M.T. Reza, J. Andert, B. Wirth, D. Busch, J. Pielert, J.G. Lynam, J. Mumme, Hydrothermal carbonization of biomass for energy and crop production, *Appl. Bioenergy* 1 (2014) 11–29, <https://doi.org/10.2478/apbi-2014-0001>.
- [11] V. Benavente, E. Calabuig, A. Fullana, Upgrading of moist agro-industrial wastes by hydrothermal carbonization, *J. Anal. Appl. Pyrol.* 113 (2015) 89–98, <https://doi.org/10.1016/j.jaap.2014.11.004>.
- [12] S.M. Heilmann, H.T. Davis, L.R. Jader, P.A. Lefebvre, M.J. Sadowsky, F. J. Schendel, M.G. von Keitz, K.J. Valentas, Hydrothermal carbonization of microalgae, *Biomass Bioenergy* 34 (2010) 875–882, <https://doi.org/10.1016/j.biombioe.2010.01.032>.
- [13] R.B. Levine, T. Pinnarat, E. Savage, Biodiesel production from wet algal biomass through in situ lipid hydrolysis and supercritical transesterification, *Energy Fuels* 24 (2010) 5235–5243, <https://doi.org/10.1021/ef1008314>.
- [14] S.M. Heilmann, L.R. Jader, L.A. Harned, M.J. Sadowsky, F.J. Schendel, P. A. Lefebvre, M.G. von Keitz, K.J. Valentas, Hydrothermal carbonization of microalgae II. Fatty acid, char, and algal nutrient products, *Appl. Energy* 88 (2011) 3286–3290, <https://doi.org/10.1016/j.apenergy.2010.12.041>.
- [15] H. Liu, Y. Chen, H. Yang, F.G. Gentili, U. Söderlind, X. Wang, W. Zhang, H. Chen, Hydrothermal treatment of high ash microalgae: Focusing on the physicochemical and combustion properties of hydrochars, *Energy Fuels* 34 (2020) 1929–1939, <https://doi.org/10.1021/acs.energyfuels.9b04093>.
- [16] C.G. Khoo, M.K. Lam, A.R. Mohamed, K.T. Lee, Hydrochar production from high-ash low-lipid microalgal biomass via hydrothermal carbonization: Effects of operational parameters and products characterization, *Environ. Res.* 188 (2020), 109828, <https://doi.org/10.1016/j.envres.2020.109828>.
- [17] A. Broch, U. Jena, S.K. Hoekman, J. Langford, Analysis of solid and aqueous phase products from hydrothermal carbonization of whole and lipid-extracted algae, *Energies* 7 (2014) 62–79, <https://doi.org/10.3390/en7010062>.

- [18] Y. Lu, R.B. Levine, P.E. Savage, Fatty acids for nutraceuticals and biofuels from hydrothermal carbonization of microalgae, *Ind. Eng. Chem. Res.* 54 (2015) 4066–4071, <https://doi.org/10.1021/ie503448u>.
- [19] U. Ekpo, A.B. Ross, M.A. Camargo-Valero, P.T. Williams, A comparison of product yields and inorganic content in process streams following thermal hydrolysis and hydrothermal processing of microalgae, manure and digestate, *Bioresour. Technol.* 200 (2016) 951–960, <https://doi.org/10.1016/j.biortech.2015.11.018>.
- [20] J. Lee, K. Lee, D. Sohn, Y.M. Kim, K.Y. Park, Hydrothermal carbonization of lipid extracted algae for hydrochar production and feasibility of using hydrochar as a solid fuel, *Energy* 153 (2018) 913–920, <https://doi.org/10.1016/j.energy.2018.04.112>.
- [21] K.Y. Park, K. Lee, D. Kim, Characterized hydrochar of algal biomass for producing solid fuel through hydrothermal carbonization, *Bioresour. Technol.* 258 (2018) 119–124, <https://doi.org/10.1016/j.biortech.2018.03.003>.
- [22] H. Liu, Y. Chen, H. Yang, F.G. Gentili, U. Söderlind, X. Wang, H. Chen, Hydrothermal carbonization of natural microalgae containing a high ash content, *Fuel* 249 (2019) 441–448, <https://doi.org/10.1016/j.fuel.2019.03.004>.
- [23] L. Garcia Alba, C. Torri, C. Samori, J. van der Spek, D. Fabbri, S.R.A. Kersten, D.W. F. Brilman, Hydrothermal treatment (HTT) of microalgae: Evaluation of the process as conversion method in an algae biorefinery concept, *Energy Fuels* 26 (2012) 642–657, <https://doi.org/10.1021/ef201415s>.
- [24] J.D. Marin-Batista, J.A. Villamil, J.J. Rodriguez, A.F. Mohamedano, M.A. de la Rubia, Valorization of microalgal biomass by hydrothermal carbonization and anaerobic digestion, *Bioresour. Technol.* 274 (2019) 395–402, <https://doi.org/10.1016/j.biortech.2018.11.103>.
- [25] M. Saber, F. Takahashi, K. Yoshikawa, Characterization and application of microalgae hydrochar as a low-cost adsorbent for Cu(II) ion removal from aqueous solutions, *Environ. Sci. Pollut. Res.* 25 (2018) 32721–32734, <https://doi.org/10.1007/s11356-018-3106-8>.
- [26] M. Mäkelä, V. Benavente, A. Fullana, Hydrothermal carbonization of lignocellulosic biomass: Effect of process conditions on hydrochar properties, *Applied Energy* 155 (2015) 576–584, <https://doi.org/10.1016/j.apenergy.2015.06.022>.
- [27] M. Volpe, J.L. Goldfarb, L. Fiori, Hydrothermal carbonization of *Opuntia ficusindica* cladodes: role of process parameters on hydrochar properties, *Bioresour. Technol.* 247 (2018) 310–318, <https://doi.org/10.1016/j.biortech.2017.09.072>.
- [28] M. Lucian, M. Volpe, L. Gao, G. Piro, J.L. Goldfarb, L. Fiori, Impact of hydrothermal carbonization conditions on the formation of hydrochars and secondary chars from the organic fraction of municipal solid waste, *Fuel* 233 (2018) 257–268, <https://doi.org/10.1016/j.fuel.2018.06.060>.
- [29] D. Knezevic, W. van Swaaij, S. Kersten, Hydrothermal conversion of biomass II. Conversion of wood, pyrolysis oil and glucose in hot compressed water, *Ind. Eng. Chem. Res.* 49 (2010) 104–112, <https://doi.org/10.1021/ie900964u>.
- [30] A. Jain, R. Balasubramanian, M.P. Srinivasan, Hydrothermal conversion of biomass waste to activated carbon with high porosity: A review, *Chem. Eng. J.* 283 (2016) 789–805, <https://doi.org/10.1016/j.cej.2015.08.014>.
- [31] M. Sevilla, W. Gu, C. Falco, M.M. Titirici, A.B. Fuertes, G. Yushin, Hydrothermal synthesis of microalgae-derived microporous carbons for electrochemical capacitors, *J. Power Sources* 267 (2014) 26–32, <https://doi.org/10.1016/j.jpowsour.2014.05.046>.
- [32] I. Bargmann, C.M. Rillig, W. Buss, A. Kruse, M. Kuecke, Hydrochar and biochar effects on germination of spring barley, *J. Agron. Crop Sci.* 199 (2013) 360–373, <https://doi.org/10.1111/jac.12024>.
- [33] F. Fornes, R.M. Belda, Acidification with nitric acid improves chemical characteristics and reduces phytotoxicity of alkaline chars, *J. Environ. Manage.* 191 (2017) 237–243, <https://doi.org/10.1016/j.jenvman.2017.01.026>.
- [34] M. Sevilla, A.B. Fuertes, The production of carbon materials by hydrothermal carbonization, *Carbon* 47 (2009) 2281–2289, <https://doi.org/10.1016/j.carbon.2009.04.026>.
- [35] X. Sun, Y. Li, Colloidal carbon spheres and their core/shell structures with noble-metal nanoparticles, *Angew. Chem. Int. Ed.* 43–597-601 (2004), <https://doi.org/10.1002/anie.200352386>.
- [36] K.D. Baugh, P.L. McCarty, Thermochemical pretreatment of lignocellulose to enhance methane fermentation: I. Monosaccharide and furfurals hydrothermal decomposition and product formation rates, *Biotechnol. Bioeng.* 31 (1988) 50–61, <https://doi.org/10.1002/bit.260310109>.
- [37] S.M. Heilmann, L.R. Jader, M.J. Sadowsky, F.J. Schendel, M.G. von Keitz, K. J. Valentas, Hydrothermal carbonization of distiller's grains, *Biomass Bioenergy* 35 (2011) 2526–2533, <https://doi.org/10.1016/j.biombioe.2011.02.022>.
- [38] R. Kothari, S. Ahmad, V.V. Pathak, A. Pandey, A. Kumar, R. Shankarayan, P.N. Black, V.V. Tyagi, 2019. Algal-based biofuel generation through flue gas and wastewater utilization: a sustainable prospective approach. *Biomass Conv. Bioref.* 10.1007/s13399-019-00533-y.
- [39] S. Lage, F.G. Gentili, Quantification and characterization of fatty acid methyl esters in microalgae: Comparison of pretreatment and purification methods, *Bioresour. Technol.* 257 (2018) 121–128, <https://doi.org/10.1016/j.biortech.2018.01.153>.
- [40] V. Samburova, M.S. Lemos, S. Hübel, S.K. Hoekman, J.C. Cushman, B. Zielinska, Analysis of triacylglycerols and free fatty acids in algae using ultra performance liquid chromatography mass spectrometry, *J. Am. Oil. Chem. Soc.* 90 (2013) 53–64, <https://doi.org/10.1007/s11746-012-2138-3>.
- [41] J.F. Saldarriaga, R. Aguado, A. Pablos, M. Amutio, M. Olazar, J. Bilbao, Fast characterization of biomass fuels by thermogravimetric analysis (TGA), *Fuel* 140 (2015) 744–751, <https://doi.org/10.1016/j.fuel.2014.10.024>.
- [42] J. Tolu, L. Gerber, J.F. Boily, R. Bindler, High-throughput characterization of sediment organic matter by pyrolysis-gas chromatography/mass spectrometry and multivariate curve resolution: A promising analytical tool in (paleo)limnology, *Anal. Chim. Acta* 880 (2015) 93–102, <https://doi.org/10.1016/j.aca.2015.03.043>.
- [43] A. Funke, F. Ziegler, Hydrothermal carbonization of biomass: A summary and discussion of chemical mechanisms for process engineering, *Biofuel Bioprod. Biorefining* 4 (2010) 160–177, <https://doi.org/10.1002/bbb.198>.
- [44] A. Kruse, F. Koch, K. Stelzl, D. Wüst, M. Zeller, Fate of nitrogen during hydrothermal carbonization, *Energy Fuels* 30 (2016) 8037–8042, <https://doi.org/10.1021/acs.energyfuels.6b01312>.
- [45] R.B. Levine, C.O.S. Sierra, R. Hockstad, W. Obeid, P.G. Hatcher, P.E. Savage, The use of hydrothermal carbonization to recycle nutrients in algal biofuel production, *Environ. Prog. Sustain. Energy* 32 (2013) 962–975, <https://doi.org/10.1002/ep.11812>.
- [46] L. Pane, E. Franceschi, L. De Nuccio, A. Carli, Applications of thermal analysis on the marine phytoplankton, *Tetraselmis suecica*, *J. Therm. Anal. Calorim.* 66 (2001) 145–154, <https://doi.org/10.1023/A:1012443800271>.
- [47] D. Busch, C. Kammann, L. Grünhage, C. Müller, Simple biotoxicity tests for evaluation of carbonaceous soil additives: establishment and reproducibility of four test procedures, *J. Environ. Qual.* 40 (2011) 1–10, <https://doi.org/10.2134/jeq2011.0122>.
- [48] C.J. Ennis, J. Clarke, K. Neate, J. Cerejeira, L. Tull, Hydrothermal extraction of microalgae fatty acid influences hydrochar phytotoxicity, *Front. Environ. Sci.* 5 (2017) 47, <https://doi.org/10.3389/fenvs.2017.00047>.
- [49] H.B. Klinka, A.B. Thomsen, B.K. Ahring, Inhibition of ethanol-producing yeast and bacteria by degradation products produced during pre-treatment of biomass, *Appl. Microbiol. Biotechnol.* 66 (2004) 10–26, <https://doi.org/10.1007/s00253-004-1642-2>.
- [50] J. Mu, Z. Yu, W. Wu, Q. Wu, Preliminary study of application effect of bamboo vinegar on vegetable growth, *Forest. Stud. China* 8 (2006) 43–47, <https://doi.org/10.1007/S11632-006-0023-6>.
- [51] N.I. Ali, I.A. Siddiqui, S. Shahid Shaikat, M.J. Zaki, Nematicidal activity of some strains of *Pseudomonas* spp, *Soil Biol. Biochem.* 34 (2002) 1051–1058, [https://doi.org/10.1016/S0038-0717\(02\)00029-9](https://doi.org/10.1016/S0038-0717(02)00029-9).
- [52] C.A. Palm, P.A. Sanchez, Decomposition and nutrient release patterns of the leaves of three tropical legumes, *Biotropica* 22 (1990) 330–338, <https://doi.org/10.2307/2388550>.
- [53] R.R. Northup, R.A. Dahlgren, J.G. McColl, N. van Breemen, Polyphenols as regulators of plant-litter-soil interactions in northern California's pygmy forest: a positive feedback, *Biogeochem.* 42 (1998) 189–220, https://doi.org/10.1007/978-94-017-2691-7_10.
- [54] G. Tian, F.K. Salako, F. Ishida, Replenishment of C, N, and P in a degraded Alfisol under humid tropical conditions: effect of fallow species and litter polyphenols, *Soil Sci.* 166 (2001) 614–621, <https://doi.org/10.1097/00010694-200109000-00005>.
- [55] V.D.S. Nunes-Halldorson, R.L. Steiner, G.B. Smith, Residual toxicity after biodegradation: interactions among benzene, toluene, and chloroform, *Ecotoxicol. Environ. Saf.* 57 (2004) 162–167, [https://doi.org/10.1016/S0147-6513\(03\)00032-0](https://doi.org/10.1016/S0147-6513(03)00032-0).
- [56] M. Hitzl, A. Mendez, M. Owsianiak, M. Renz, Making hydrochar suitable for agricultural soil: A thermal treatment to remove organic phytotoxic compounds, *J. Environ. Chem. Eng.* 6 (2018) 7029–7034, <https://doi.org/10.1016/j.jece.2018.10.064>.
- [57] K.A. Spokas, J.M. Novak, C.E. Stewart, K.B. Cantrell, M. Uchimiya, M.G. DuSaire, K.S. Ro, Qualitative analysis of volatile organic compounds on biochar, *Chemosphere* 85 (2011) 869–882, <https://doi.org/10.1016/j.chemosphere.2011.06.108>.